Available online at www.sciencedirect.com
ScienceDirect
C. R. Physique 7 (2006) 1082–1100
COMPTES RENDUS PHYSIQUE
http://france.elsevier.com/direct/COMREN/

Nucleation/Nucléation

Dew nucleation and growth

Daniel Beysens [a,b]

[a] *Laboratoire de physique et mécanique des milieux hétérogènes, CNRS – ESPCI – université Paris 6 et Paris 7, 10, rue Vauquelin, 75231 Paris cedex 05, France*

[b] *Équipe du supercritique pour l'environnement, les matériaux et l'espace, service des basses températures, Commissariat à l'énergie atomique de Grenoble, 38054 Grenoble cedex 9, France*

Available online 28 November 2006

Abstract

Dew is the condensation of water vapor into liquid droplets on a substrate. It is characterized by an initial heterogeneous nucleation on a substrate and a further growth of droplets. The presence of a substrate that geometrically constrains the growth is the origin of the peculiarities and richness of the phenomenon. A key point is the drop interaction through drop fusion or coalescence, which leads to scaling in the growth and gives universality to the process. As a matter of fact, growth dynamics are only dependent on substrate and drop dimensionality. Coalescence events lead to temporal and spatio-temporal fluctuations in the substrate coverage, drop configuration, etc., which give rise to a very peculiar dynamics. When the substrate is a liquid or a liquid crystal, the drop pattern can exhibit special spatial order, such as crystalline, hexatic phases and fractal contours. Condensation on a solid substrate near its melting point can make the drop jump.

The applications of monitoring dew formation are manifold. Examples can be found in medicine (sterilization process), agriculture (green houses) and hydrology (production of drinkable water). ***To cite this article: D. Beysens, C. R. Physique 7 (2006).***

Résumé

Nucléation et croissance de buée et rosée. La rosée se forme par condensation de vapeur d'eau sur un substrat sous forme de gouttelettes. Elle se caractérise par une nucléation hétérogène des gouttelettes suivie par leur croissance. La présence du substrat, qui induit une contrainte géométrique durant cette croissance, est à l'origine des particularités et de la richesse du phénomène. Le point important est l'interaction des gouttes par fusion ou coalescence, qui conduit à une croissance auto-similaire et lui assure son universalité. La dynamique de croissance ne dépend en effet que de la dimensionnalité du substrat et de celle des gouttes. Les coalescences mènent à des fluctuations temporelles et spatio-temporelles dans la couverture de substrat, dans la configuration des gouttes, etc., qui est à l'origine d'une dynamique très particulière. Quand le substrat est un liquide ou un cristal liquide, l'arrangement des gouttes peut montrer un ordre spatial spécial, tel que des phases cristalline et hexatique et des contours fractals. La condensation sur un substrat solide, près de son point de fusion peut faire « sauter » les gouttes. Les applications qui découlent du contrôle de la formation de la buée ou de la rosée sont diverses. On peut citer des exemples en médecine et en biologie (stérilisation), dans l'agriculture (serres) en hydrologie (production d'eau potable). ***Pour citer cet article : D. Beysens, C. R. Physique 7 (2006).***

Keywords: Nucleation; Heterogeneous nucleation; Dew; Breath figures; Dropwise condensation; Coalescence; Wetting

Mots-clés : Nucléation ; Nucléation hétérogène ; Rosée ; Condensation en gouttes ; Coalescence ; Mouillage

E-mail address: daniel.beysens@espci.fr (D. Beysens).

1631-0705/$ – see front matter
doi:10.1016/j.crhy.2006.10.020

1. Introduction

Everybody knows what is dew—this natural phenomenon where humid air condenses on a substrate and transforms into liquid water. However, its occurrence in nature has long been a mystery as it is precisely when the sky is free of clouds that dew forms. Dew looks to crop up from nowhere. W.H. Wells was the first, at the beginning of the 19th century, to elaborate a reasonable understanding of its formation [1]. It is only in the middle of the 20th century that a precise theory has been proposed [2]. For meteorologists, dew water is not considered as a precipitation, like rain, as it depends on the substrate where it forms (it is considered as the inverse of evaporation). For hydrologists, dew can be a potential source of water [3]. For the botanist, dew participates in a plant's exchange with the atmosphere [4]. Dew can also be an unfavorable phenomenon; dew on plant leaves enables spores, and especially fungus spores, to develop, a phenomenon to be avoided [5]. The formation of dew on green-house shields lowers the light transmission by more than 50% [6,7] and so limits the yield of agricultural production. In biology, dew nucleates preferentially on micro-organisms, because they are hydrophilic. The addition of bactericide substances soluble in water gives to dew extended sterilization properties [8]. In the laboratory, dew is often called 'breath figures' [9,10] for obvious reasons.

For the physicist, dew is essentially a problem of phase transition: a bulk homogeneous phase, characterized by its temperature and pressure, transforms in a liquid phase on a substrate held at a lower temperature. (The presence of another gas, nitrogen or air, does not modify fundamentally the problem of condensation.) What makes this situation attractive is the interplay of three important actors: the substrate, whose geometry constrains the growth of the dew droplets on a surface of lower dimensionality than the drops, the wetting properties, which will decide whether condensation is drop or filmwise, and the condensing phase thermodynamics. The constraint is two-dimensional (2D) if the substrate is a plane, one-dimensional (1D) if it is a line or a thread. The case of a zero-dimensional substrate corresponds to a point-like heterogeneity, as in fog or rain formation. More complicated micropatterned geometry with controlled wetting properties of the substrate correspond to superhydrophobic surfaces.

2. Heterogeneous nucleation

If a vapor is subject to a pressure p_r larger than its saturation pressure p_s (or a temperature lower than its saturation temperature), it is in a metastable state and will eventually condense into a liquid phase, its state of minimal energy. In the time sequence of formation of a liquid droplet, the first event is the formation (*nucleation*) by thermal fluctuations of the smallest nucleus—a liquid drop—that is thermodynamically stable, i.e. does not evaporate. The change in energy for a volume V of vapour that transforms into liquid is $W = -\Delta e V$ (Δe is the change in volumic free energy). However, the energy of formation $S\gamma$ of the liquid–vapour interface (here γ is the liquid–vapour interfacial tension and S is the droplet surface area) is an energy barrier to cross. The total energy balance W that is needed to transform a fluctuation of size R or volume V ($= \frac{4\pi}{3}R^3$) with a spherical liquid droplet of same volume is thus

$$W = -\frac{4\pi R^3}{3}\Delta e + 4\pi R 2\gamma \tag{1}$$

The energy cost W exhibits a maximum

$$W_{\max} = \frac{16\pi}{3}\frac{\gamma 3}{\Delta e^2} \tag{2}$$

for a 'critical' radius R^*

$$R^* = \frac{2\gamma}{\Delta e} \tag{3}$$

This maximum work therefore shows that the liquid drop is stable only for a radius $R > R^*$. The associated nucleation rate (the number dn of droplets of radius R^* that has nucleated during the time dt) corresponds to the probability that a thermal fluctuation gains $W_{\max}$. As the formation of liquid droplets is a thermally activated process, one gets

$$\frac{\mathrm{d}n}{\mathrm{d}t} \sim \exp\left(-\frac{W_{\max}}{kT}\right) \tag{4}$$

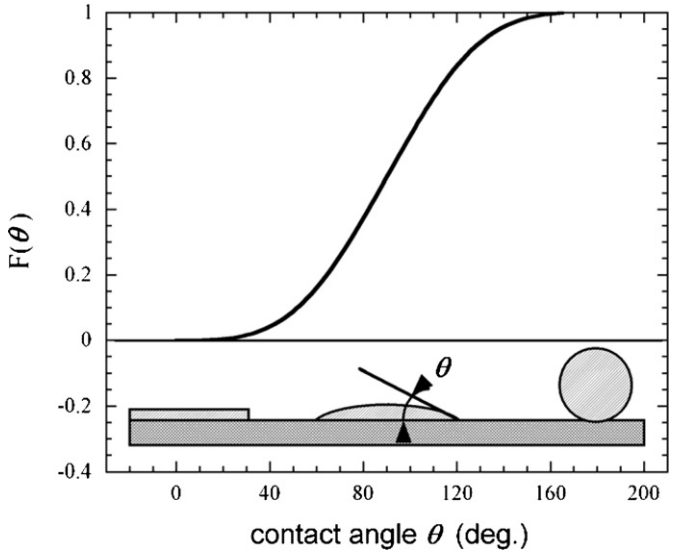

Fig. 1. Contact angle variation of $F(\theta)$, the cost of energy to form a nucleus on a substrate, relative to the bulk case (see text). Complete drying and bulk case: $\theta = 180°$; partial wetting: $180° > \theta > 0$; complete wetting: $\theta = 0$.

Fig. 1. Variation de $F(\theta)$, le coût en énergie pour nucléer un objet sur une surface, par rapport au cas en volume (voir le texte). Séchage complet et situation en volume : $\theta = 180°$; mouillage partiel : $180° > \theta > 0$; mouillage complet : $\theta = 0$.

By making use of the Clapeyron formula (ideal gas), Δe can be expressed in terms of p_s and p_r [11] and the above formulation can be written as:

$$\frac{\mathrm{d}n}{\mathrm{d}t} = B \exp\left(-\frac{16\pi}{3(kT)^3} \frac{\gamma^3 v_0^2}{\log^2 \frac{p_r}{p_s}} \right) \tag{5}$$

Here k is the Boltzmann constant, B is a numerical constant of order 10^{25} cm^{-3} s^{-1} that provides the link between the molecular scale and the macroscopic (experimental) scale; v_0 is the molar volume. The exponential behavior corresponds to a very sharp change when p_r is varied. Such a variation is, for instance, made by varying temperature. When the exponential reaches unity, nucleation starts. For example, saturated water vapor at 20 °C would condense only around 0 °C, with a critical radius $R^* \approx 30$ Å (see e.g. [12]).

However, daily experience shows that dew forms at much higher temperature. This is because condensation occurs on a substrate whose surface properties lower or even suppress the cost of forming the interface. Such a nucleation is called 'heterogeneous', in contrast to condensation which occurs in the bulk, which is called 'homogeneous'. The energy barrier indeed depends on the wetting properties of the substrates. Wetting is characterized by the contact angle θ drop-substrate (Fig. 1). The contact angle is zero for complete wetting (water forms a wetting film), and maximum for a liquid droplet that does not wet the substrate (complete drying). The maximum work to obtain a stable nucleus is thus modified through a θ-dependent function that accounts for the volume of the spherical cap and the surfaces of the cap and its base. According to Volmer [11,13], it results in a modification of the nucleation rate, Eq. (5), as

$$\frac{\mathrm{d}n}{\mathrm{d}t} = B \exp\left(-\frac{16\pi}{3(kT)^3} \frac{\gamma^3 v_0^2}{\log^2 \frac{p_r}{p_s}} F(\vartheta) \right) \tag{6}$$

with

$$F(\theta) = \left(\frac{1 - \cos\theta}{2} \right)^2 (2 + \cos\theta) \tag{7}$$

For $\theta < 180°$, the nucleation rate is always higher than for homogeneous nucleation. Heterogeneous nucleation therefore permits condensation for temperature differences much less than that required for homogeneous nucleation [14] (see also Section 4.4 and Fig. 6 where the contact angle is continuously varied). In addition, defects of the substrate (scratches, chemicals, etc.) play the role of very large fluctuations and favor nucleation.

The dew point temperature is the temperature at which $p_r = p_s$. In terms of the classical psychometric (Mollier) humid-air diagram for water, the relative humidity (p_s/p_r) is 100%. Just below the dew point temperature the nucleation rate, although finite, is extremely small. Experimentally speaking, it is then only on completely wetted substrate that condensation can be observed at the dew point.

Because of unavoidable contamination (e.g. by human manipulation), substrates that are not specially protected or designed are covered with fatty substances that make the contact angle water-substrate to be around 40–90° ($\theta = 0°$ on ultra clean glass). This is why 'dew' is most often the result of the condensation of water into tiny droplets, which scatter light and make dew appear 'white' and are at the origin of the current troublesome optical problems encountered with dew. This dropwise condensation contrasts with filmwise condensation, optically nearly invisible.

The fact that nucleation is favored by wetting conditions has important implications. In Section 8, this property is used in biological sterilization.

3. Growth of an isolated droplet

Once a droplet of water has nucleated on the substrate, it grows at the expense of the surrounding atmosphere (Fig. 2). We restrain our study to the case where a constant flux of molecules is brought to the surface, i.e. the atmosphere exhibits a constant velocity U parallel to the substrate [15]. Liquid will condense on the surface and a depletion region, which we take to be stagnant, will be established near the wall. If the concentration of water in the gas stream is small, w, the rate of mass transfer per unit area normal to the wall, is given by [16]

$$w = D_{12}(p_r - p_s)/\delta_0 RT \tag{8}$$

where D_{12} is the diffusion constant of water in the carrier gas, R is the gas constant, T is the mean temperature and δ_0 is the thickness of the depletion layer.

To evaluate δ_0, we consider the wall as a flat plate on which there is a temperature discontinuity. In this case, the depletion-layer thickness can be related to the free-stream velocity U, the kinematic viscosity μ and the Schmidt number $Sc = \mu/D_{12}$ by [17]

$$\delta_0 = \frac{(x\mu/U)^{1/2}}{CSc^{1/3}} \tag{9}$$

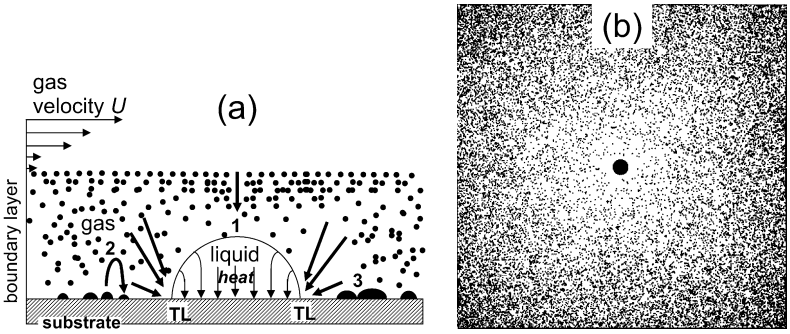

Fig. 2. Growth of a single drop. (a) A gas saturated in water is sent on a substrate, with velocity U. In the quiescent boundary layer, water molecules diffuse to the substrate. Different processes can concur to the growth of the drop: (1) direct accommodation at the drop surface, with release of latent heat leading to a maximum temperature gradient at the line of three phase contact TL; (2) nucleation and evaporation of clusters of near critical radius, resulting in a surface diffusion towards the drop; (3) nucleation, growth and coalescence of small droplets. (b) Numerical simulation of the process. The drop (black, in the center) incorporates a constant flux of monomers diffusing from the sides. The drop radius grows as $t^{1/3}$. (From [15].)

Fig. 2. Croissance d'une goutte unique. (a) Un gaz saturé d'eau est envoyé sur un substrat, avec la vitesse U. Dans la couche limite, les molécules d'eau diffusent vers le substrat. Différents processus peuvent concourir à la croissance de la goutte : (1) incorporation directe à la surface de la goutte, avec dégagement de chaleur latente menant à un gradient de température maximal à la ligne de contact des trois phases TL ; (2) nucléation et évaporation d'agrégats de rayon à-peu-près critiques, diffusant ainsi vers la goutte ; (3) nucléation, croissance et coalescence de petites gouttelettes. (b) Simulation numérique du processus. La goutte (noire, au centre) incorpore un flux constant de monomères qui diffusent à partir des côtés. Le rayon de la goutte croît comme $t^{1/3}$. (Tiré de [15].)

In this expression x is the distance traveled past the edge of the temperature discontinuity and C is a constant, of order 0.33 [18].

Combining Eqs. (8), (9) gives an expression for the dependence on the flow rate of the time t_f required to deposit a fixed amount of material on the surface

$$1/t_f \sim w \sim \sqrt{U^*}(p_r - p_{s)} D_{12} \tag{10}$$

where $U^* = U/\mu D_{12}^{1/3}$. (Note that usually the flow rate is expressed in terms of the volumetric flow $F = UA_S$, or scaled flow rate $F^* = U^* A_S$, where A_S is the cross-sectional area of the flow stream.)

At the lowest flow rates, the depletion model cannot work as δ becomes comparable to the cell height; all the water can condenses and $t_f^{-1} \sim F$.

In order to get rid of the flow rate and supersaturation dependence, one can thus use the reduced time

$$t^* = t/t_f \sim t\sqrt{F^*}\,(p_r - p_{s)} D_{12} \tag{11}$$

In a steady state of condensation, the volume $V \sim R^3$ of a liquid drop of radius R is proportional to time as,

$$V \sim t \tag{12}$$

or

$$R \sim t^{\mu_s} \tag{13}$$

with $\mu_s = 1/3$.

A complication may arise when the latent heat of condensation cannot be released into the substrate. In this case, the temperature of the drop increases; its growth is slowed down and can even stop. This is especially the case for very fast growth when the air velocity is large. In such conditions the 'effective' growth law exponents which are measured satisfy $\mu_s < 1/3$ [15,19]. Note that the above analysis does not imply a precise knowledge of the microscopic mechanisms of growth. Several competing mechanisms can be considered (Fig. 2):

(i) Direct accommodation of water molecules at the drop surface. A temperature gradient is formed due to the release of the latent heat. This release makes the perimeter of the drop, where the gradient is maximum, the place where the mass transport (accommodation of water molecules) is also a maximum.
(ii) The thermal release of energy at the surface of the drop induces temperature gradients parallel to the liquid–vapor interface which, in turn, can induce flows through buoyancy. (Thermocapillary Marangoni flows [20] cannot be initiated by the gradient of surface tension at the interface liquid–vapor as the latter is isothermal.) This internal hydrodynamics is effectively observed for very fast growth where small particles inside the drop undergo very fast motion.
(iii) Nucleation of drops of critical radius that grow and fuse and eventually reach the drop where they are incorporated [15,19,21–23]. This leads to a drop size distribution that is observed only during the late stages of growth.
(iv) Nucleation and evaporation on the substrate, resulting in a surface diffusion that feeds the drop at its perimeter [24].

The perimeter of the drop (the 3-phase contact line) appears to play a key role for the growth process, whatever are the mechanisms involved. This fact is experimentally verified in the following (see below, Section 6.3 and Fig. 11).

4. Growth of a droplet pattern

Two drops can interact by fusion or coalescence because they grow and touch at their perimeter. These interactions by coalescence are geometrically constrained by the substrate: 2-dimensional interactions for a planar substrate, the most common case, one-dimensional interactions for a line, as threads in a spider web, more complex interactions for patterned substrates, etc.

After coalescence, a new drop is formed whose volume is the sum of the volumes of the initial drops. The formation of a new single drop is favorable in terms of energy since the surface area, and then the surface energy, is lowered by the coalescence event. The center of mass of the new drop is approximately at the center of mass of the two

'parents'. Coalescence has the remarkable consequence of leaving free room on the substrate for further condensation and growth. If one considers e.g. two hemispherical 'parent' drops with same radius, covering the total surface area

$$2A = 2\pi R^2 \tag{14}$$

the area A' of the new droplet is equal to

$$A' = 2^{2/3}\pi R^2 \tag{15}$$

and is lower than the surface coverage of the parents, $A'/A = 2^{-1/3} \approx 80\%$. (The drop grows in the third dimension.)

This property of releasing surface after coalescence is at the origin of a constant surface coverage during the drop pattern evolution. This constant coverage is a hall-mark of the self-similarity of the growth. It is quite general as it is based on the difference in dimensionality between the drop (dimensionality D_d) and the substrate (dimensionality D_s). Quite generally, surface release occurs when the ratio

$$D_s/D_d < 1 \tag{16}$$

Self-similarity is not altered if surface defects pin the perimeter of the drop as coalescence always decreases the wet surface on the substrate, thus still leading to a constant surface coverage.

Several stages of growth can be characterized. They depend on the interactions between the droplets as will be seen now.

4.1. Growth without significant interactions

This first stage, which occurs after nucleation has occurred, is characterized by a low surface coverage (Fig. 3). (The surface coverage ε is the ratio: surface area covered by the drops/substrate area.) Only a very few coalescence events occur and the mean droplet radius of the pattern $\langle R\rangle$ grows as for a single drop (Eq. (13)):

$$\langle R\rangle \sim t^{\mu_s} \tag{17}$$

4.2. Self-similar regime

In this regime the pattern evolution remains self-similar in time and exhibits universal features (Figs. 4(a), (b)). It happens when the surface coverage typically exceeds 30%, which leads to important interactions by coalescence between the droplets.

The first obvious effect of coalescence is the speeding-up of the growth, as shown in Figs. 3(a), (b). The second effect is the stabilization of the surface coverage to a constant (and 'universal', see [25,28]) value, $\varepsilon_\infty \approx 55\%$ for hemispherical drops (Fig. 3(c)). The constancy of ε is the result of two opposite effects: continuous condensation tends to produce an increase in the droplets radii and thus in ε, resulting in turn to an increase in the number of coalescences, which in contrast lowers ε. The balance for hemispherical drops is not very far from the 2D random packing limit, i.e., the packing obtained when disks of same radius are randomly sent on a plane where no overlapping is allowed. The constancy of ε leads to the apparent paradox of a continuous increase of the condensed mass at constant surface coverage—which implies that growth also occurs in the third dimension.

This constant surface coverage is the hall-mark of the self-similarity of the pattern evolution. By self-similarity we mean that the average characteristics of a pattern at time t_i (Fig. 4(a)) are identical (statistically speaking) to those of a pattern at time t_j (Fig. 4(b)) provided that all distances are expressed in units of the average droplet radius $\langle R(t_j)\rangle$ (pattern at t_j) and $\langle R(t_i)\rangle$ (pattern at t_i).

During this regime, the time dependence of $\langle R\rangle$ (Fig. 3(b)) is still a power law [26]:

$$\langle R\rangle \sim t^{\mu_a} \tag{18}$$

with the growth law exponent that is deduced from the single drop growth exponent μ_a as

$$\mu_a = \mu_s \frac{D_d}{D_d - D_s} \tag{19}$$

For ideal thermal conditions, $\mu_s = 1/D_d$ and

$$\mu_a = \frac{1}{D_d - D_s} \tag{20}$$

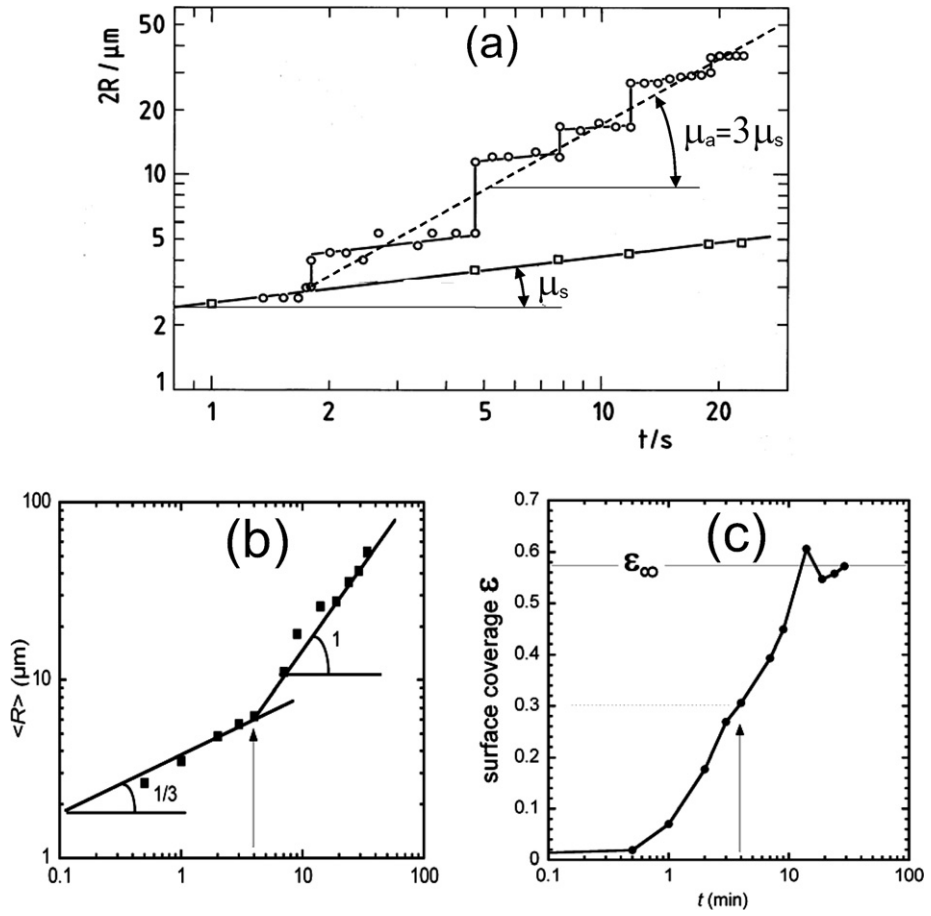

Fig. 3. (a) Evolution of the radius of a droplet in a pattern. The lower line (squares) corresponds to a growth where the effect of coalescence has been removed. Coalescences strongly accelerate the growth (upper line, circles), the growth law exponent is multiplied by 3, in accordance with Eq. (19). (From [19].) (b)–(c) Evolution of the mean radius $\langle R\rangle$ of the drop pattern and of the drop surface coverage ε. When $\varepsilon < 0.3$, the drops have no interactions, the growth exponent is μ_s $(= 1/3)$. When $\varepsilon > 0.3$, the drops have strong interactions by coalescence, the growth exponent becomes $3\mu_s$ $(= 1)$. The arrow shows the limit between the two regimes.

Fig. 3. (a) Évolution du rayon d'une gouttelette dans un ensemble. La ligne inférieure (carrés) correspond à une croissance où l'effet des coalescences a été suprimé. Les coalescences accélèrent fortement la croissance (ligne supérieure, ronds) et l'exposant de la loi de croissance est multiplié par 3, selon l'Eq. (19). (Tiré de [19].) (b)–(c) Evolution du rayon moyen $\langle R\rangle$ de l'ensemble de gouttes et de la fraction de surface ε mouillée par celles-ci. Quand $\varepsilon < 0.3$, les gouttes n'ont aucune interaction, l'exposant de croissance est μ_s $(= 1/3)$. Quand $\varepsilon > 0.3$, les gouttes subissent de fortes interactions par coalescence, l'exposant de croissance devient $3\mu_s$ $(= 1)$. La flèche montre la limite entre les deux régimes.

For the usual situation where the drop is three-dimensional and the substrate is a plane ($D_d = 3$, $D_s = 2$) and

$$\mu_s = 1/3, \qquad \mu_a = 1 \tag{21}$$

The growth is considerably accelerated by the coalescences, as already noted (Figs. 3(a), (b)).

A striking demonstration (Fig. 5) of the relevance of the above scaling theory is made by analyzing the formation of dew on a iris leaf [27]. The leaf is formed of joint fibers of 15 µm diameter covered with cutin, a vegetal wax on which water makes drops with 90° contact angle. The drops nucleate preferentially on the fibers and grow firstly without interactions (they are too far away to touch and coalesce), with the exponent $\mu_s = 1/D_d = 1/3$. They then interact on the fibers as long as the drop diameter does not exceed that of the fibers. The interaction between drops is here 1D and the exponent of growth should be $\mu_a = 1/(D_d - D_s) = 1/2$. When the drops become much larger than the fiber diameter, their interaction is 2D, which gives $\mu_a = 1/(D_d - D_s) = 1$. On Fig. 5, one clearly sees the different growth laws, with the exponents $1/3$, $1/2$ and 1.

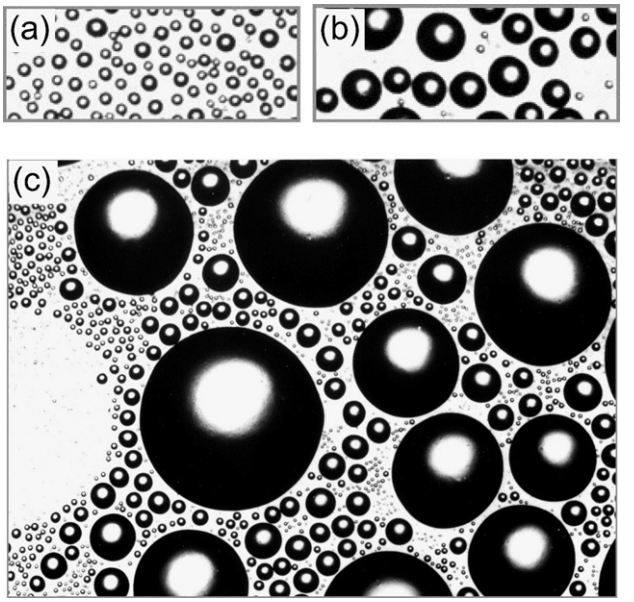

Fig. 4. Self-similar growth of a pattern of droplets condensing on hydrophobic glass (treated by silanization). The pattern at $t = 1$ s (a) after condensation started, is equivalent to the one at $t = 6$ s (b). In (c), at $t = 25$ s, new families of droplets have nucleated between the initial drops. When taken separately, these families all present the self-similar properties of the first generation. (Photo (c): Briscoe and Galvin, 1989.)

Fig. 4. Croissance auto-similaire d'un ensemble de gouttes se condensant sur du verre (traité hydrophobe par silanisation). L'ensemble de gouttes à $t = 1$ s (a) après le début de la condensation, est équivalent à celui à $t = 6$ s (b). En (c), à $t = 25$ s, de nouvelles familles de gouttelettes ont nucléé entre les gouttes initiales. Prises séparément, ces familles présentent les mêmes propriétés d'auto-similarités de la première génération. (Photo (c) : Briscoe et Galvin, 1989.)

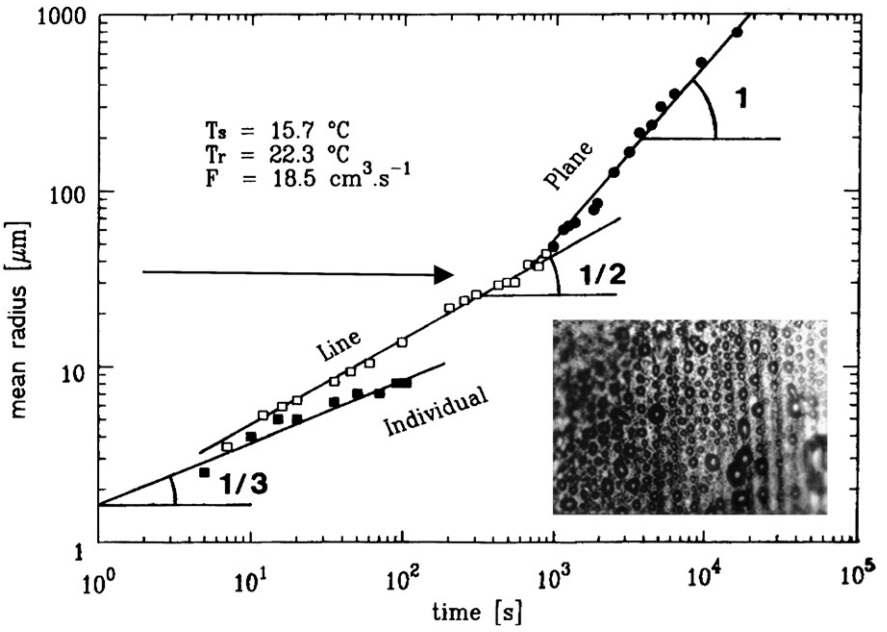

Fig. 5. Evolution of the droplet pattern shown in the insert (photo). The mean droplet radius grows firstly without interactions (exponent 1/3), then the drops interacts on a line (exponent 1/2) and eventually interacts on a plane (exponent 1), when the diameter of the drops exceeds the fiber thickness (arrow). The width of the photo is 285 μm. (From [27].)

Fig. 5. Évolution de l'ensemble de gouttelette montré dans l'insert (photo). L'évolution du rayon moyen des gouttelettes correspond d'abord à une croissance sans interactions (exposant 1/3), puis les gouttes interagissent sur une ligne (exposant 1/2) et finalement sur un plan (exposant 1), quand le diamètre des gouttes excède la largeur des fibres (flèche). La largeur de la photo est 285 μm. (Tiré de [27].)

An interesting property is the formation of correlations between the drops due to coalescence. These correlations are obvious as no drops can lie in a circle of radius of order on $2\langle R\rangle$ without being incorporated, see Fig. 4. The pair correlation function of drops looks like that of a liquid, with a well-defined peak at the distance $2\langle R\rangle$ corresponding to the nearest neighbors [28]. The presence of well-defined correlations somewhat increases the surface coverage from the random packing limit. (This effect is particularly important for growth on a 1D substrate where the measurement gives $\varepsilon = 80\%$, to be compared to the random packing limit 75% [27].) Note that the drop polydispersity, which could also explain the increase in surface coverage, remains however small and constant ($\approx 18\%$) during the self-similar growth [15,28].

4.3. Steady state and gravity effects

Depending on the experimental conditions, new tiny droplets can nucleate on the space left free after coalescence. These droplets form a new 'family', which exhibits all the features (growth laws, surface coverage) of the first generation of droplets. After a while the substrate appears to be covered by a whole range of families (Fig. 4(c)). Although the surface coverage exhibits the same (universal) value for each family, the total surface coverage increases, however to a value that will never reach unity.

Gravity matters when the drops size becomes of the order of the water capillary length

$$l_c = \sqrt{\frac{\gamma}{g\delta\rho}} \tag{22}$$

Here g is the gravitational acceleration ($\approx 10\ \mathrm{m\,s^{-2}}$), γ is the water-air interfacial tension ($\approx 70\times 10^{-3}\ \mathrm{J\,m^{-2}}$) and $\delta\rho$ is the density difference between air and liquid water ($\approx 103\ \mathrm{kg\,m^{-3}}$). Gravity then matters when $l_c \gtrsim 2.5$ mm at room temperature. Gravity causes the drops larger than a few mm to flatten and eventually flow. Then a new generation of droplets can nucleate on the free surface. A steady state can thus be reached, with continuous formation of new droplet patterns and flow of the largest drops. In the steady state, the distribution of the droplet radius obeys a power law

$$n(R) \sim R^{-y} \tag{23}$$

with $y \approx 2.7$ [29]. (This power law has not been studied in absence of gravity, when the drops cannot flow.)

In industrial condensers, this 'dropwise' condensation gives a better yield than film condensation because of the enhanced heat transfer at the perimeter of the drops. However, impurities cannot be avoided after a while, causing pinning of the drops which eventually form an irregular, pseudo-wetting film (Fig. 6, bottom line).

4.4. Effects of the substrate heterogeneity

The above stages can be altered because the substrate is not perfect [25]. The chemical heterogeneities have the effect of changing the contact angle and modifying the nucleation rate according to Eqs. (6), (7); this is particularly obvious on Fig. 6, left column, where the number of nucleation sites increases when the contact angle decreases. Geometrical heterogeneities can also pin the perimeter of the drops, an effect which is particularly visible when the contact angles are small, corresponding to a weak restoring force after coalescence. This force is $\gamma(\cos\theta_{\mathrm{eq}} - \cos\theta)$, with θ the dynamic contact angle—the smaller at coalescence—and θ_{eq} the final equilibrium contact angle (see [30] and the discussion below in 4.5). The drop that results from the coalescence of two drops is not hemispherical any more; it looks rather a cigar or even a more complicated shape (Fig. 6). Since the surface area of the new droplet is always lower than the sum of the surface areas of the two 'parents', self-similarity can be preserved (right column). However, the surface coverage increases to reach asymptotically unity when the contact angle θ goes to zero, following approximately [25]

$$\varepsilon_\infty \approx 1 - 0.005\theta \tag{24}$$

with θ in degrees.

4.5. Coalescence and contact line dynamics

For sessile drops coalescence, the contact line motion influences strongly the coalescence kinetics. Coalescence phenomenon is basically a two stage process: (i) the nucleation of a bridge between the drops (Fig. 7(a)) and the

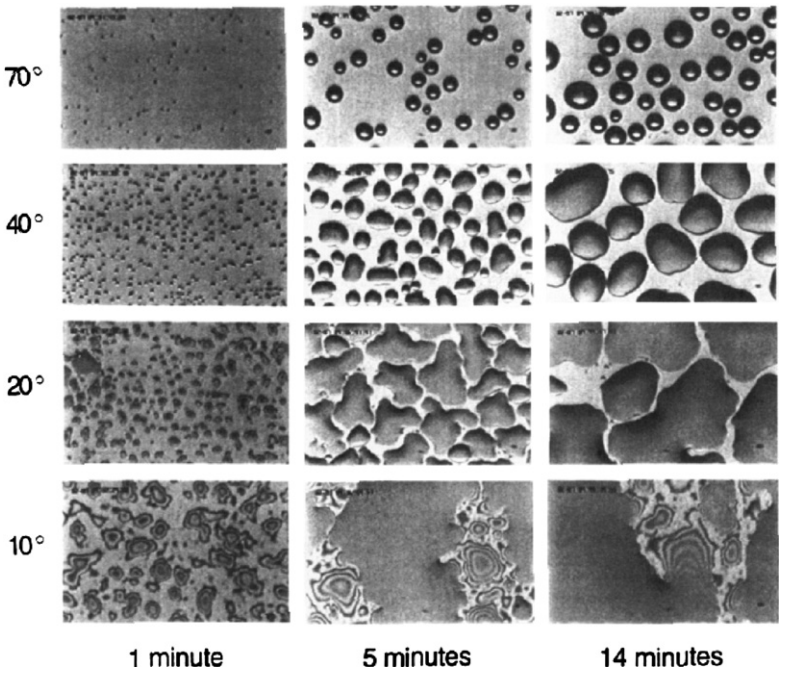

Fig. 6. Examples of growth patterns of water condensing on cold silicon wafer with a coating providing a gradient of contact angle [25]. Each column represents the patterns obtained at 4 different locations on the substrate. The width of the photo is 385 μm. (From [25].)

Fig. 6. Exemples de gouttes d'eau se condensant sur une plaquette de silicium refroidie et traitée pour obtenir un gradient d'angle de contact [25]. Chaque colonne représente le motif obtenu à 4 endroits différents du substrat. La largeur de la photo est 385 μm. (Tiré de [25].)

formation of an elongated, composite drop (Fig. 7(b)); and (ii) the relaxation of the composite drop to a near circular shape, where the contact line motion plays a key role (Figs. 7(c), (d)). The relaxation of the composite drop for water [30,31] and diethylene glycol [32] (160 times more viscous than water) leads to the same conclusion: the relaxation time is 10^7 times larger than the bulk capillary relaxation as an effect of the contact line dynamics.

The theories of contact line dynamics (see e.g. [33,34] and references therein) results into a general expression for the contact line velocity u_n in the direction normal to the contact line:

$$u_n = \frac{\gamma}{\xi}(\cos\theta_{\text{eq}} - \cos\theta) \tag{25}$$

Here ξ is a model dependent parameter called the 'contact line dissipation coefficient'. Another aspect of these theories is that they predict a very large ξ value when compared to the shear viscosity η so that ξ/η is much larger than unity. This high dissipation can be associated to an Arrhenius factor resulting from the phase change in the contact line vicinity [33] and to the influence of surface defects that pin the contact line [34].

5. Fluctuations

In the self-similar regime, the surface coverage is a constant only on average. Fluctuations occur that are correlated with the coalescence events (Fig. 8(a)). Interesting information can be provided from the space-time variation of these events.

5.1. Temporal fluctuations

Fluctuations can be of temporal nature. Let us consider the set of coalescence events for a particular droplet. One marks a droplet by a dye which is incorporated into the new droplets resulting from the successive coalescences (Fig. 9(a)). It can be shown [35] that the number of coalescences $N(t)$ before time t varies as

$$N \sim \ln t \tag{26}$$

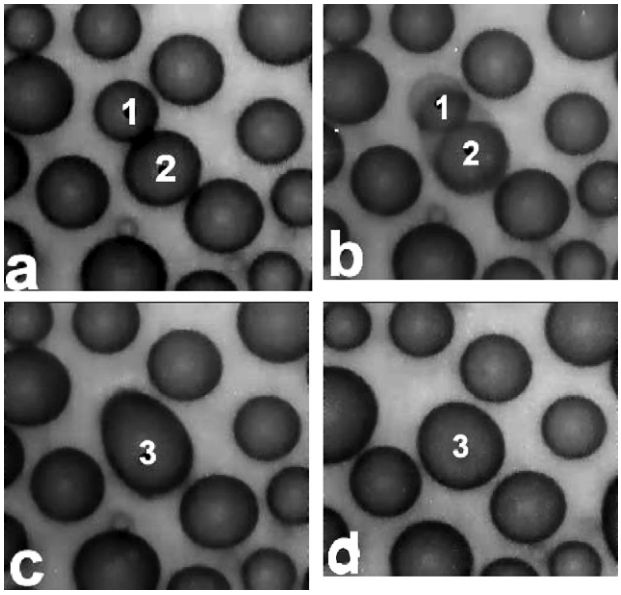

Fig. 7. Photos of the coalescence process. The side of each photo corresponds to 276 μm. (a) $t = 5.59$ s; (b) $t = 5.63$ s; (c) $t = 5.65$ s; (d) $t = 42.76$ s. (From [30].)

Fig. 7. Photos du processus de coalescence. Le coté de chaque photo correspond à 276 μm. (a) $t = 5.59$ s ; (b) $t = 5.63$ s ; (c) $t = 5.65$ s ; (d) $t = 42.76$ s. (Tiré de [30].)

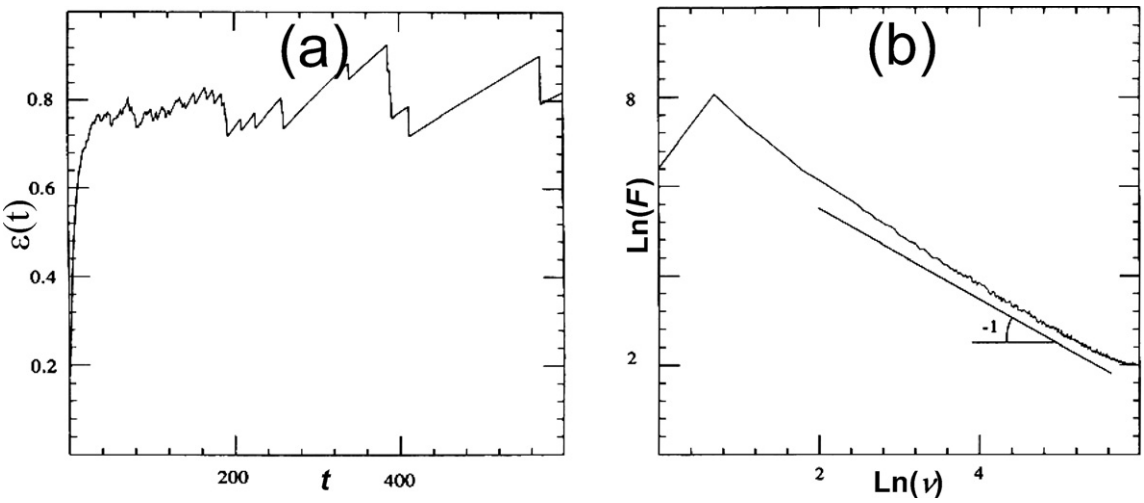

Fig. 8. (a) Evolution of the surface coverage $\varepsilon(t)$ in a simulation of 3D droplet growing on a 1D substrate. (b) Fourier transform modulus of the coverage $\varepsilon(t)$ shown in (a); ν is frequency. (Log–log plot; from [36].)

Fig. 8. (a) Evolution de la fraction de surface $\varepsilon(t)$ couverte par les gouttes dans une simulation de gouttelettes 3D croissant sur un substrat 1D. (b) Module de la transformée de Fourier de la surface couverte $\varepsilon(t)$ montrée en (a) ; ν est la fréquence. (Coordonnées log–log ; tiré de [36].)

This logarithmic law leads to a large slow down of the coalescence frequency with time. If one considers a particular drop at time t, the next coalescence will occur in average only after a time $\Delta t \approx t$.

These coalescence events make the surface coverage vary. Fluctuations in coverage exhibit a noise which is typical of dropwise condensation and depends neither of the dimensionality of the drops nor on that of the substrate. The amplitude of the Fourier transform shows a $1/\nu$ dependence (ν is the temporal frequency)—or equivalently the power spectrum obeys a $1/\nu^2$ dependence, without any cut-off (Fig. 8(b)). This is, to our knowledge, the only example known in physics of such frequency dependence [36].

5.2. Spatio-temporal fluctuations

The fluctuations in time and space of the droplet configuration obey a particular behavior. Let us mark a droplet which has nucleated (e.g. by a dye, as noted above), follow its fate (Fig. 9(a)) and study how the dye spreads over the substrate by the growth and coalescence of the droplets. This is interesting in the case where 'active' (i.e., fluorescent or chemically active) particles are incorporated initially into a droplet, and one would like to know how these particles spread out in space.

The important parameters are, in addition to the number of coalescences, N, the mean displacement δ of the drop center at time t (Fig. 9(a)).

The result concerning δ is relatively obvious if one realizes that the mean displacement is ruled by the last coalescence, which imposes a motion of the centers over a distance on order R (Fig. 9(a)):

$$\sqrt{\langle \delta^2 \rangle} \sim R(t) \tag{27}$$

Another interesting question is concerned with the study of the collective properties of the pattern, and especially how the ensemble of droplets collectively wets the substrate. One can suppose that the droplets are the condensation of a product which decontaminates the substrate [35]. The question which then arises is to know which fraction f—called the 'dry' fraction of the substrate—has not yet been touched by the droplets at any previous time. This fraction has not

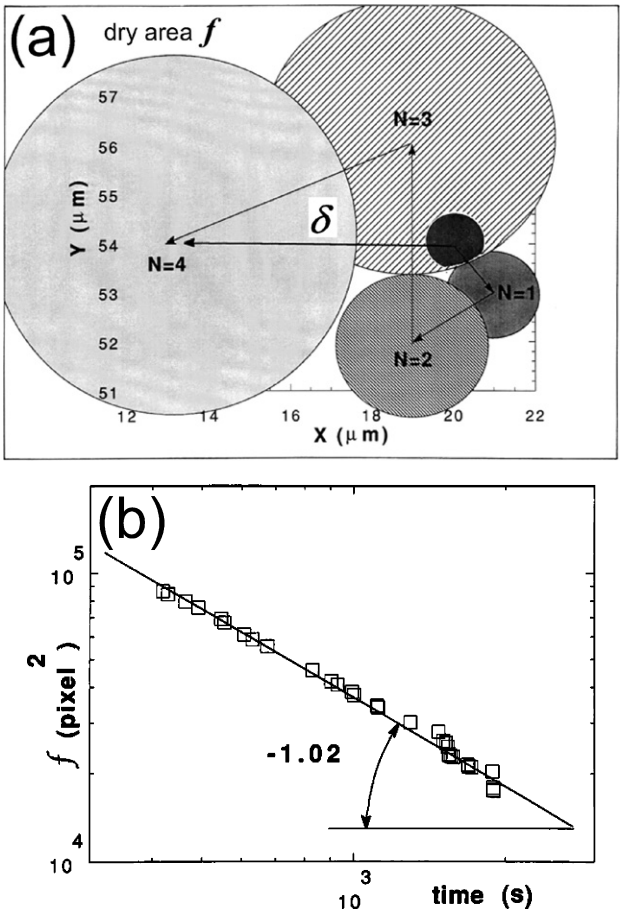

Fig. 9. (a) How a dye spreads over a substrate thanks to the growth and coalescence of droplets (see text). (b) Evolution of the 'dry' area f (substrate area never touched by a drop). (From [35].)

Fig. 9. (a) Comment un colorant s'étale sur un substrat du fait de la croissance et de la coalescence des gouttelettes (voir le texte). (b) Evolution de la fraction « sèche » f (fraction du substrat jamais touché par une goutte). (Tiré de [35].)

to be confused with the fraction $1 - \varepsilon_\infty$ (≈ 0.45 for hemispherical drops, see Eq. (24)) that is dry at a given instant of time. It appears that f decreases as a power law,

$$f \sim t^{-\alpha} \tag{28}$$

with $\alpha \sim 1$. This exponent can be obtained from simply assuming that the different drop configurations before and after each coalescence are independent [35]. It anticipates the well known 'persistence exponents' [37].

6. Non solid substrates

6.1. Liquid substrates

Water droplets can nucleate and grow on a liquid surface. A typical experiment is concerned with the flat, horizontal surface air/paraffin oil [38–41]. The surface of a liquid is smooth up to the size of the thermally-induced capillary fluctuations, making, for chemically cleaned surfaces, nucleation sites less numerous than on a solid surfaces. The first stage of growth, as discussed in the previous Sections 2 and 3 above, is thus markedly longer than for solid substrates.

Since water is denser than paraffinic oil, water droplets should sink unless their weight is counterbalanced by surface tension forces. This induces a deformation of the air/oil interface which, in turn, causes elastic long-ranged attractive forces between droplets (in 1/distance). The droplets, however, do not coalesce immediately, in contrast to those growing on a solid substrate, because the film of oil that separates them has to dissipate. The thinning of such films is a slow process, whose velocity decreases with the film thickness. The droplets can therefore arrange themselves in typical hexagonal, two-dimensional 'crystals'. These crystals in turn attract each other and rotate to align their symmetry axes. In this process holes are formed, and the structure that appears is typical of two-dimensional crystal melting, it forms a 'hexatic' phase (Fig. 10), a phase characterized by an orientational order but no translational order. At a larger scale, the structure of the pattern of islands forms what is called a 'fat fractal' [41].

When the drops become too large and fill all the surface, they start to coalesce and the pattern of droplets becomes similar to that observed with solids, with the same growth law. The structure is, however, more ordered since the liquid substrate permits an easy local rearrangement of the drops.

6.2. Liquid crystals

A liquid crystal in its nematic phase is a liquid formed of highly anisotropic molecules where a high orientational order is observed. In particular, these molecules orientate perpendicularly to the interface water/liquid crystal. When dew forms on such a liquid crystal, one observes the condensation of drops. As for a regular liquid, these drops do not coalesce immediately. Surprisingly, the drops order into parallel lines, which even form 'zig-zag' configurations. The reason is that the surface air/liquid crystal is deformed by the water drops. This causes long-ranged, anisotropic interactions of dipolar type between the drops. One of the possible configurations of such dipoles in interaction is precisely the observed pattern.

After a while, the same phenomenon as for a liquid substrate occurs: coalescence starts, and a pattern alike that observed on a liquid substrate is formed, with the same evolution laws.

6.3. Solid near its melting point

Let us consider now a solid near its melting point, like cyclohexane below 6.7 °C. During condensation from water at room temperature, the growth of the droplets is accompanied by furious movements of rotation, translation and hopping [42]. Microscopic observation shows that the substrate melts along the line of three-phase contact, solid–liquid–vapor (Fig. 11), because of the release in the substrate of the latent heat of condensation. When analyzing the typical time dependence of these movements with the flow rate of incoming vapor and the cyclohexane temperature, one comes to the conclusion that the droplets are set into motion by the change of contact angle liquid–solid/liquid–molten solid [43] (Fig. 11). This experiment demonstrates that it is indeed at the perimeter of the drop that the mass and heat exchange are at maximum during condensation.

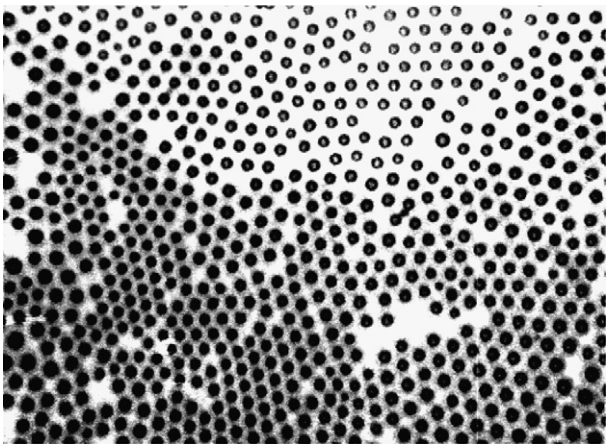

Fig. 10. Pattern of droplets at the surface of paraffinic oil, forming a two-dimensional 'hexatic' phase. The smallest dimension of the photo is 350 μm. (From [41].)

Fig. 10. Ensemble de gouttelettes à la surface d'huile de paraffine, formant une phase « hexatique » bidimensionnelle. La plus petite dimension de la photo est 350 μm. (Tiré de [41].)

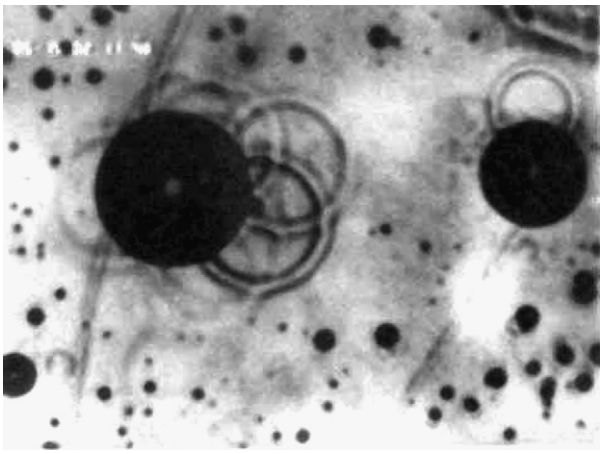

Fig. 11. Photograph of water droplets condensing on cyclohexane just above its melting point. The diameter of the largest drop is 10 μm. This drop has just performed three jumps. The positions previously occupied are marked by rings corresponding to the contact line. (From [42].)

Fig. 11. Photographie de gouttelettes d'eau se condensant sur du cyclohexane juste au-dessus de son point de fusion. Le diamètre de la plus grande goutte est 10 μm. Cette goutte vient d'exécuter trois sauts. Les positions précédemment occupées sont repérées par des anneaux correspondant à la ligne de contact. (Tiré de [42].)

7. Superhydrophobic patterned substrates

On a square patterned, superhydrophobic substrate such as that shown in Fig. 12, characterized by the pattern lengthscales ($a, b \approx d, c$), the growth of the droplet whose radius reaches and exceeds a, b, c, leads to a sequence of very unusual behavior, as displayed on Fig. 13.

During the early stages, the drop sizes remain indeed smaller than the typical length scales of the surface pattern and drops basically visit a plane surface. During the late stages, the drop size is much larger than the typical length scales of the surface pattern. Superhydrophobicity can hold only in this stage. It can be observed either the classical [44] Cassie–Baxter (or air pocket) state, where air remains trapped below the drop, generally a metastable state, or the Wenzel state, where the inter-pillar space below the drop is filled with liquid, generally the more stable state, or the penetration state, where the liquid is sucked into the inter-pillar space and also fills a region of the substrate around the drop. In the cross-over stage where $2R \approx a, b$, the drops grow over the air present in incompletely filled channels in a metastable Cassie–Baxter state. This is a quite unexpected situation that is exclusively due to the possibility of droplet bridging between pillars, a condition that resumes in $c > b$. In addition, a phenomenon of self-drying takes place when $2R > a, b, c$. This phenomenon (Fig. 2(a), $t = 86.32$ min) is similar to the drying of the top of 2D grooved surfaces [45] and is due to the coalescence of the drop on the pillars with the drops and bridges that grow in the channels. It is the expected transition from Cassie–Baxter to the most stable Wenzel state. After the drying stage, the

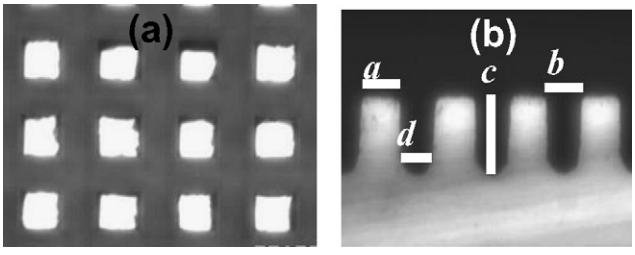

Fig. 12. Square pillar pattern silicon substrate. (a) Top view; (b) side view ($a = 32$ μm, $b = 32$ μm, $c = 62$ μm, $d = 22$ μm).

Fig. 12. Motif d'un substrat de silicium en forme de pilier carré. (a) Vue de haut ; (b) vue de coté ($a = 32$ μm, $b = 32$ μm, $c = 62$ μm, $d = 22$ μm).

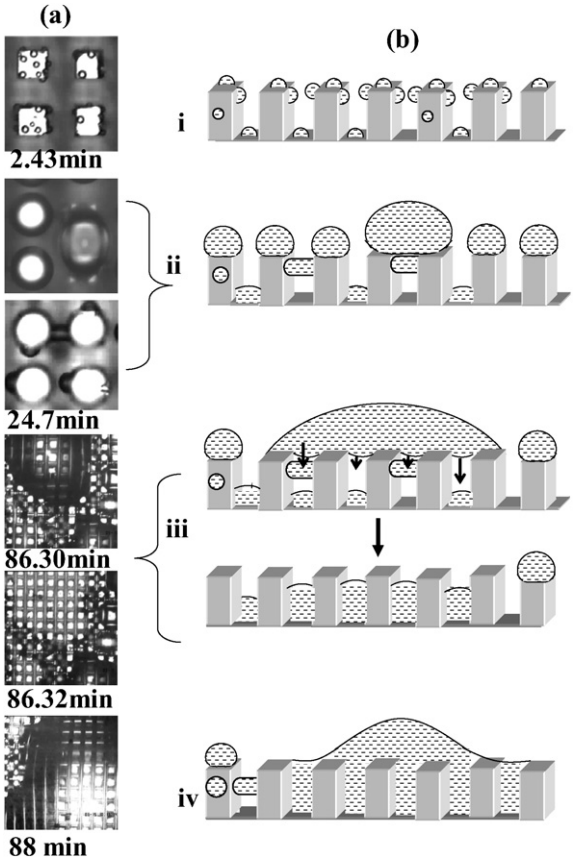

Fig. 13. (a) Time sequence of different growth stages of condensed water drops on a superhydrophobic square pillar substrate: (i) Initial (nucleation) stage ($2R < a, b, c$); (ii) Bridge formation stage ($2R \approx a, b$); (iii) Drying stage ($2R > a, b, c$); (iv) Large drop formation stage ($2R \gg a, b, c$). (b) Sketch of growth stages. (From [51].)

Fig. 13. (a) Différentes étapes de croissance de gouttes d'eau se condensant sur un substrat superhydrophobe de piliers carrées : (i) Étape initiale (nucléation) ($2R < a, b, c$) ; (ii) Étape de formation de ponts ($2R \approx a, b$) ; (iii) Étape de séchage ($2R > a, b, c$) ; (iv) Étape de formation de grande gouttes ($2R \gg a, b, c$). (b) Schéma des étapes de croissance. (Tiré de [51].)

water level in the channel increases up to the top surface and coalesces with drops at the top to form a very large drop (Fig. 13(a), stage (iv), $t = 88$ min), almost flat and having a very strong hysteresis contact angle. Its growth law compares well with that for a single drop on a flat surface $R \sim t^{1/3}$. The large drops are in a mixed Wenzel-penetration regime (the most stable state for this surface).

Some interesting features of superhydrophobicity are still present since the tops of pillars that are not covered by large drops remains almost dry. These phenomena can easily be generalized to surface geometries similar to pillars (columns, etc.).

8. Biological sterilization

A significant application of the enhanced nucleation properties of dew at surface defects is the possibility to sterilize a medical instrument or even a hospital surgery room by steam and chemical vapors including strong oxidants (O_3, H_2O_2, ...). Sterilization occurs in the liquid phase, precisely where preferential nucleation occurs on the microorganisms and/or the tissues that host them [8] (Fig. 14). The interest is manifold: as only the contaminated part of the surface is wet by the chemical, only a small amount of sterilizing chemical is used, preventing damaging the delicate instruments. It also then becomes possible to monitor a condensation-induced sterilization with only a small number of well controlled physical parameters. In addition sterilization can occur at room temperature or below.

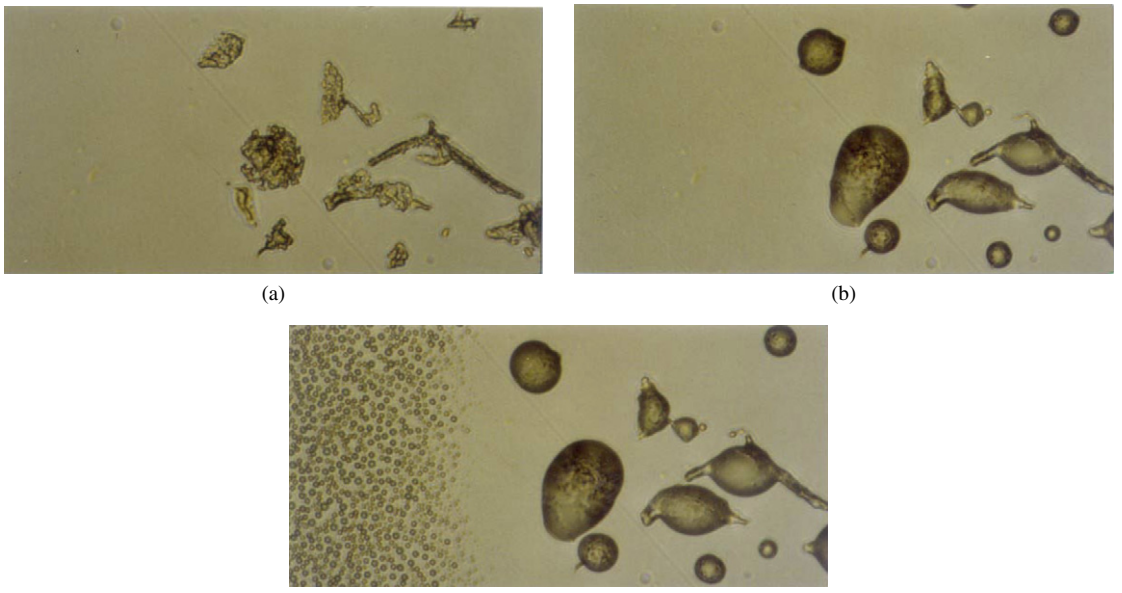

(a) (b)

(c)

Fig. 14. Lyophilized spores of Bacillus Macerans on silanized glass at room temperature (18 °C) under continuous flow of condensing vapor at 37 °C. (a) time $t = 0$, dry spores. (b) $t = 0.5$ s, the spores are wet by the condensed liquid. (c) $t = 3$ s, the clean glass starts to be covered with droplets. Condensation continues on the spores, hampering the nucleation of new droplets.

Fig. 14. Spores lyophilisées de Bacillus Macerans sur du verre silanisé à température ambiante (18 °C) sous écoulement continu de vapeur à 37 °C. (a) $t = 0$, spores sèches. (b) $t = 0{,}5$ s, les spores sont mouillées par le liquide condensé. (c) $t = 3$ s, le verre propre commence à être couvert de gouttelettes. La condensation continue sur les spores, empêchant la nucléation de nouvelles gouttelettes.

9. Harvesting dew as drinkable water

Pure water begins to be a rare substance. Using the phenomenon of condensation to collect the water contained in the atmosphere is not a new idea, but up to now, its setting up was difficult, sometimes expensive and often not very effective [3,46,47].

Several theories for dew condensation has been formulated, the first complete one by Monteith [2]. For the functioning of these condensers it has been developed the following approach [3]. Condensation proceeds from the balance between the radiative cooling energy, which cools down the condenser till the dew point temperature and compensates the release of latent heat during condensation, and heating by diffusion and convection in the environment. Radiation cooling is maximum in the atmospheric window between 8 and 16 μm wavelengths and for angles above 15° above the horizon. The available cooling power ranges between 25 and 150 $\mathrm{W\,m^{-2}}$, which gives a practical limit to dew yields to about 0.8 mm/day in the ideal case where all this energy is used to condense the vapor, i.e. to compensate for the latent heat of condensation (2500 $\mathrm{J\,g^{-1}}$ at 20 °C).

Several parameters have to be accounted for (Fig. 15): temperature T_s of the substrate, its specific heat c_c, and its mass M, which gives the thermal inertia of the condenser, the specific heat c_w and mass m of the condensed water, cooling flux by radiation R_i (day and night), heating flux by radiation R_{he} (day: Sun), heating flux due to the latent heat of condensation (R_{cond}).

The energy balance can be written as

$$\frac{\mathrm{d}T_s}{\mathrm{d}t}(Mc_c + mc_w) = R_i + R_{\mathrm{he}} + R_{\mathrm{cond}} \tag{29}$$

What enters also in the model is the condensation rate, $\mathrm{d}m/\mathrm{d}t$, which is a function of T_s, atmosphere temperature T_a, windspeed, air relative humidity, etc., according to the laws of dew formation as discussed above.

Dew yields can be enhanced by materials that behave as a black body in the atmospheric window and are totally reflective elsewhere, with hydrophilic properties to facilitate nucleation and dew recovery by gravity flows (tilted material). The material which is currently developed is based on a foil that is composed of a matrix polyethylene

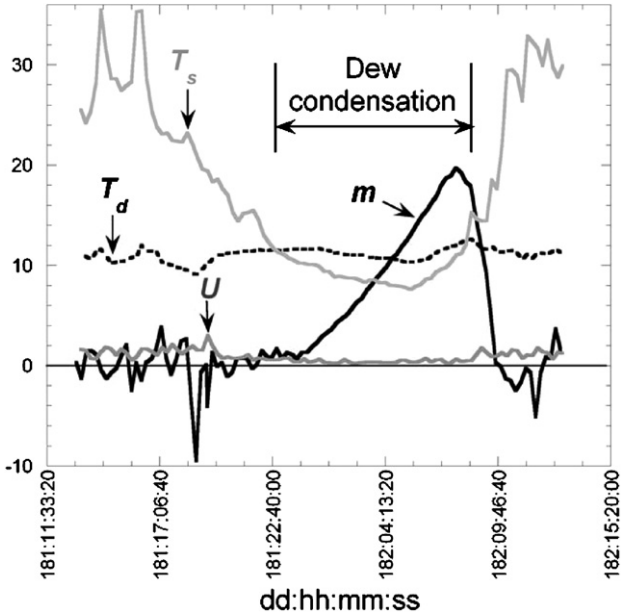

Fig. 15. Condensation of water on a substrate of 0.16 m^2 at 1 m above the ground over one day. The period of condensation (production of the water m mass is in g) occurs when the temperature of the surface (T_S, in °C) is lower than the dew point temperature (T_d, in °C). U is the wind speed expressed in m/s, measured at 1 m above the ground.

Fig. 15. Condensation d'eau sur un substrat de 0,16 m^2 à 1 m au-dessus du sol durant une journée. La période de condensation (production de masse d'eau m est en g) se produit quand la température de la surface (T_S, en °C) reste inférieure à la température de point de rosée (T_d, en °C). U est la vitesse du vent exprimée en m/s, mesuré à 1 m au-dessus du sol.

charged in microballs of oxide titanium (TiO_2) and sulphate barium ($BaSO_4$) [48] to ensure a good radiative capacity in the infra-red to which are added surface-active and anti-ultra-violin to resist solar radiations UV, especially in summer periods.

The investigations are carried out in Ajaccio (France, University of Corsica) and throughout the world under supervision of OPUR [49] (France, Croatia, India—where a dew plant is under construction—, French Polynesia, Ethiopia, Morocco, ...). They show the effectiveness and the simplicity of implementation of the device (Fig. 16), dew harvesting giving a significant amount of water, sometimes comparable to rain.

Chemical and bacteriological studies on dew water [50] have shown that it is in general drinkable (standards of quality imposed by the World Health Organization and the European directive into force) after a filtration, limiting the turbidity of water, and disinfection, for safety reasons as the collectors are in the open air.

10. Concluding remarks

What one would expect from the above studies of dew is the control of its formation. Several industrial processes can indeed be described by the different stages of formation of dew as e.g. the first stages of thin film growth by vapor deposition. When the interest is water collection, dew water is welcome and can give a significant amount of water. On other occasions, it can be just the opposite; dew has to be suppressed (on spectacles, car windshields, green houses, etc.). Canceling durably the effect of dew is still a major industrial challenge.

It appears that dew can be controlled by two key parameters: temperature and the wetting properties of the substrate. These two parameters control the nucleation rate and the latter has in addition major consequences on the form and growth of the droplet pattern. The wetting properties of a substrate can be easily modified by surface treatments. This is an advantage, but also an inconvenience. Contamination alters dramatically the wetting properties, and especially fatty contamination, unavoidable in a human environment. (Even a monolayer of fat can change the contact angle of water on glass from 0° to 100°.) In this aspect, micropatterned (superhydrophobic) substrates can give up to now only a limited solution as the final state is always the most stable Wenzel state where the drops are pinned on the substrate.

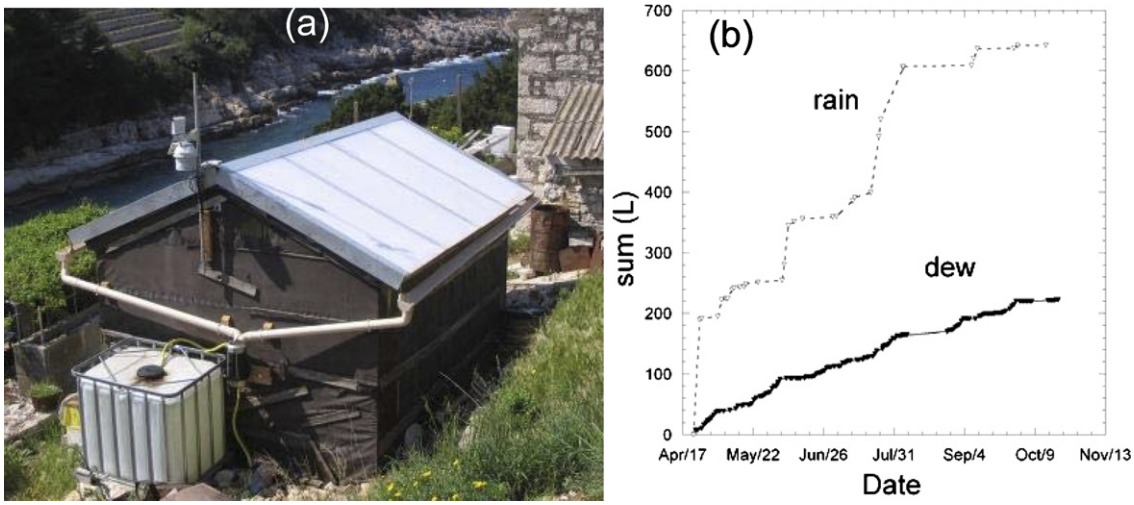

Fig. 16. (a) A 15 m^2 roof equipped to collect dew (Island of Biševo, Adriatic Sea, Croatia). (b) Dew and rain recovery during 6 months (preliminary data). (From [52].)

Fig. 16. (a) Un toit de 15 m^2 équipé pour collecter la rosée (île de Biševo, mer Adriatique, Croatie). (b) Récupération de rosée et de pluie comparée sur 6 mois (données préliminaires). (Tiré de [52].)

Acknowledgements

I thank V. Nikolayev and J. Villain for a critical reading of the manuscript.

References

[1] W.H. Wells, An Essay on Dew, and Several Appearances Connected with It, Taylor and Hessey, London, 1814.
[2] J.L. Monteith, Dew. Q. J. Royal Meteorol. Soc. 83 (1957) 322–341.
[3] V. Nikolayev, D. Beysens, A. Gioda, I. Milimouk, E. Katiushin, J.-P. Morel, J. Hydrology 182 (1996) 19–35.
[4] J.-P. L'Homme, O.F. Jimenez, Agricultural and Forest Meteorology 62 (1992) 263–274.
[5] L. Huber, T.J. Gillepsie, Ann. Rev. Phytopath 30 (1992) 553–577.
[6] A. Jaffrin, S. Makhlouf, C. Scotto la Massese, A. Bettachini, R. Voisin, Agronomie 9 (1989) 729–741.
[7] B. Briscoe, K. Galvin, J. Solar Energy 46 (1991) 191–197.
[8] M.A. Marcos-Martin, A. Bardat, R. Schmitthaeusler, D. Beysens, Pharm. Technol. Eur. 8 (1996) 24–32.
[9] T.J. Baker, Philos. Mag. 44 (1922) 752.
[10] R. Merigoux, Rev. Opt. 9 (1937) 281.
[11] L.D. Landau, E.M. Lifshitz, Statistical Physics, Pergamon Press, London–Paris, 1958.
[12] N.N. Das Gupta, S.K. Gosh, Rev. Mod. Phys. 18 (1946) 223–290.
[13] M. Volmer, Kinetic der phasebildung, Th. Steinkopff, Dresden and Leipzig, 1939.
[14] S. Twomey, J. Chem. Phys. 30 (1959) 941–943.
[15] D. Fritter, C.M. Knobler, D. Beysens, Phys. Rev. A 43 (1991) 2858–2869.
[16] F. Kreith, Principles of Heat Transfer, third ed., Harper and Row, San Francisco, 1973.
[17] In analogy to heat transfer, see R.J. Nickerson, in: W.R. Rohsenow (Ed.), Developments in Heat Transfer, MIT Press, Cambridge, MA, 1964, p. 37.
[18] L.E. Sissom, D.R. Pitts, Elements of Transport Phenomena, McGraw–Hill, San Francisco, 1972, p. 522.
[19] D. Beysens, C.M. Knobler, Phys. Rev. Lett. 57 (1986) 1433–1436.
[20] J.K. Platten, J.C. Legros, Convection in Liquids, Springer-Verlag, Berlin, 1984.
[21] A. Steyer, P. Guenoun, D. Beysens, C.M. Knobler, Phys. Rev. A 44 (1991) 8271–8277.
[22] F. Family, P. Meakin, Phys. Rev. Lett. 61 (1988) 428–431.
[23] P. Meakin, Rep. Prog. Phys. 55 (1992) 157–240.
[24] T.M. Rogers, K.R. Elder, R.C. Desai, Phys. Rev. A 38 (1988) 5303–5309.
[25] H. Zhao, D. Beysens, Langmuir 11 (1995) 627–634.
[26] J.L. Viovy, D. Beysens, C.M. Knobler, Phys. Rev. A 37 (1988) 4965–4970.
[27] A. Steyer, P. Guenoun, D. Beysens, D. Fritter, C.M. Knobler, Europhys. Lett. 12 (1990) 211–215.
[28] D. Fritter, C.M. Knobler, D. Roux, D. Beysens, J. Stat. Phys. 52 (1988) 1447–1459.
[29] J.W. Rose, L.R. Glicksman, Int. J. Heat Mass Transfer. 16 (1972) 411–425.

[30] C. Andrieu, D.A. Beysens, V.S. Nikolayev, Y. Pomeau, J. Fluid Mech. 453 (2002) 427–438.
[31] R. Narhe, D. Beysens, V.S. Nikolayev, Langmuir 20 (2004) 1213–1221.
[32] D.A. Beysens, R.D. Narhe, J. Phys. Chem. B 110 (2006) 22133–22135.
[33] Y. Pomeau, C. R. Acad. Sci. Paris, Ser. IIb 238 (2000) 411–416.
[34] V.S. Nikolayev, J. Phys. Condens. Matter 17 (2005) 2111–2119.
[35] M. Marcos-Martin, D. Beysens, J.-P. Bouchaud, C. Godrèche, I. Yekutieli, Physica A 214 (1995) 396–412.
[36] A. Steyer, P. Guenoun, D. Beysens, Phys. Rev. Lett. 68 (1992) 1869–1871.
[37] See e.g. A. Baldassarri, J.P. Bouchaud, I. Dornic, C. Godrèche, Phys. Rev. E 59 (1999) R20–R23, and references therein.
[38] A. Brin, R. Mérigoux, C. R. Acad. Sci. (Paris) 238 (1954) 1808–1809.
[39] C.M. Knobler, D. Beysens, Europhys. Lett. 6 (1988) 707–712.
[40] A. Steyer, P. Guenoun, D. Beysens, C.M. Knobler, Phys. Rev. B 42 (1990) 1086–1089.
[41] A. Steyer, P. Guenoun, D. Beysens, Phys. Rev. E 48 (1993) 428–431.
[42] A. Steyer, P. Guenoun, D. Beysens, Phys. Rev. Lett. 68 (1992) 64–66.
[43] J.I. Katz, Phys. Rev. E 49 (1994) 914–915.
[44] See e.g. A. Lafuma, D. Quéré, Nat. Mat. 2 (2003) 457, and references therein.
[45] R.D. Narhe, D.A. Beysens, Phys. Rev. Lett. 93 (2004) 076103.
[46] I. Mylymuk, D. Beysens, A la poursuite des fontaines aériennes, Book-eBook, Sofia–Antipolis, 2005.
[47] D. Beysens, I. Milimouk, V. Nikolayev, S. Berkowicz, M. Muselli, B. Heusinkveld, A.F.G. Jacobs, J. Arid Env. 67 (2006) 343–352.
[48] T. Nilsson, Sol. Energy Mat. Sol. Cells 40 (1996) 23–32.
[49] http://www.opur.u-bordeaux.fr.
[50] D. Beysens, C. Ohayon, M. Muselli, O. Clus, Atm. Env. 40 (2006) 3710–3723.
[51] R. Narhe, D. Beysens, Langmuir (2006), in press.
[52] D. Beysens, O. Clus, M. Mileta, I. Milimouk, M. Muselli, V.S. Nikolayev, Energy (2006), in press.